Effusion Cooling Plates for Combustor Liners: Experimental and Numerical Investigations on the Effect of Density Ratio

Available online at www.sciencedirect.com

ScienceDirect

Energy Procedia 45 (2014) 1402 – 1411

Energy Procedia

68th Conference of the Italian Thermal Machines Engineering Association, ATI2013

Effusion cooling plates for combustor liners: experimental and numerical investigations on the effect of density ratio

Luca Andrei[a,*], Antonio Andreini[a], Cosimo Bianchini[a], Gianluca Caciolli[a], Bruno Facchini[a], Lorenzo Mazzei[a], Alessio Picchi[a], Fabio Turrini[b]

[a]*Department of Industrial Engineering, University of Florence, via di Santa Marta 3 - 50139, Florence, Italy*
[b]*Combustion System Office, Avio Aero, via Primo Maggio 56, 10040 Rivalta di Torino (TO), Italy*

Abstract

Effusion cooling represents the state-of-the-art of liner cooling technology for modern combustors. The present paper describes experimental tests aiming at evaluating the cooling performance of a multi-perforated plate in real engine representative fluid-dynamic conditions. Adiabatic effectiveness maps were obtained following the mass transfer analogy by the use of Pressure Sensitive Paint. In addition, a CFD campaign was performed in order to benchmark the reliability in estimating the cooling performance of effusion cooling liners. In order to include anisotropic diffusion effects, the $k-\omega$ SST turbulence model was corrected considering a tensorial definition of the eddy viscosity with an algebraic correction to dope its stream-span components.

Selection and peer-review under responsibility of ATI NAZIONALE

Keywords: effusion cooling; adiabatic effectiveness; algebraic anisotropic correction; turbulence modeling; PSP technique

1. Introduction

Future aeroengines combustion devices will operate with very lean mixtures in the primary combustion zone, switching as much as possible to premixed flames. In this kind of engine the amount of air for the primary zone grows significantly at the expense of liner cooling air, which thus needs to be reduced. Consequently, important attention must be paid to the appropriate design of the liner cooling system, in order to optimize coolant consumption and guarantee an effective liner protection. All these issues have been addressed by Avio Aero. in the development of its annular combustor based on PERM (*Partial Evaporation and Rapid Mixing*) lean burn injection system. An alternative solution to typical cooling system is the full coverage film cooling or effusion cooling, which consists of a large amount of small tilted holes homogeneously distributed over the whole surface of the liner. Even if this solution still relies on film cooling generation, it permits to lower the wall temperature reducing the coolant consumption, thanks to heat removal operated by the passage of the coolant through the holes (*heat sink effect*) [1,2]. In the open literature, several studies were carried out to understand the thermal behaviour of effusion cooling schemes since the late 60's; many of these have been focused on measuring or estimating the film effectiveness generated by coolant

* Corresponding author. Tel.: +39-055-479-6618 ; fax: +39-055-479-6342.
E-mail address: luca.andrei@htc.de.unifi.it

1876-6102
Selection and peer-review under responsibility of ATI NAZIONALE
doi:10.1016/j.egypro.2014.01.147

jets [3,4]. Recently Ligrani et al.[5] presented film effectiveness and heat transfer results for full coverage film cooling arrangements with streamwise pressure gradient; they studied the effect of the blowing ratio and the influence of dense and sparse hole arrays on the thermal effectiveness.

Despite many experimental studies deal with investigating the effusion cooling performance, most of them were conducted using air as coolant and mainflow, precluding the possibility to point out the effects of density ratio between the two flows. Density ratio is, however, a key parameter for the design of a combustor liner cooling system, mainly because of the actual large temperature difference between coolant and burned gases inside the core. Lin et al.[7] investigated both experimentally and numerically adiabatic film cooling effectiveness of four different inclined multihole film cooling configurations; the survey, which was specific for combustor liner applications, was performed using a mixture of air and CO_2 as coolant, but it was mainly focused on studying the influence of hole geometrical parameters and *BR* on film cooling rather than on the effects of *DR*. Andreini et al.[8] studied through an extensive experimental campaign the effect of density ratio on the cooling performance of a real engine cooling scheme composed by a slot cooling, an effusion array and a large dilution hole. They found that in penetration regime the effect of density ratio on the adiabatic effectiveness can be neglected.

The availability of accurate and reliable turbulence models for JCF computation with RANS approach is still a very challenging activity to help in the design and optimization of real cooling systems. In the last years several works have dealt with this objective. A pioneering approach in this field is the concept of directional eddy viscosity early introduced by Bergeles et al.[16] to take into account the anisotropy of turbulent field in JCF. The idea is to use a tensorial definition of eddy viscosity where the terms responsible for jet lateral diffusion are augmented through a correction factor determined by higher order simulations (DNS data). A first attempt to extend the concept of directional eddy viscosity to other turbulence models was carried out by Cottin et al.[17] where the idea of Bergeles was implemented in a $k-\omega$ SST model with a benchmarking on a typical combustor liner effusion cooling geometry. Further contribution to this family of models comes from Li et al.[18] where in the tensorial definition of eddy viscosity a set of general purpose shape functions obtained by higher order computations are used. Moreover, such formulations are derived for steady state analysis hence are valid for the mean fields only. The works of Walters[19] and Holloway et al.[15] propose a set of models, both for steady and unsteady RANS analysis, based on a local isotropic modification of eddy viscosity, with a correction factor evaluated through a dedicated transport equation. The low computational cost, with respect to DNS and LES models, makes RANS approach with anisotropic correction potentially interesting for design of modern combustor liner cooling systems. As a consequence, this model must be widely tested especially in effusion cooling situations where multiple jets interactions are present.

To the authors knowledge, in the available literature there is not present an effusion test case composed by an appreciable number of rows of holes with highly detailed adiabatic effectiveness measurements, performed in engine representative blowing and density ratio under high free turbulence conditions. A similar test case represents a severe benchmark for the numerical models that have to cope with complex turbulent flowfield and mixing phenomena due to the multiple coolant injections.

The aim of this work is the measurement of the adiabatic effectiveness of a multi-perforated plate in order to point out the effect of the blowing rate and density ratio, procuring a severe test case to stress the deficiencies of numerical models. Low and high blowing ratio conditions, corresponding respectively to the mass addiction and penetration regimes [20] are investigated and the effect of jet superposition is studied as well. The measurements were performed using the Pressure Sensitive Paint technique. Experimental results are used to validate the numerical approach: simulations were performed implementing the algebraic anisotropic correction to the standard $k-\omega$ SST turbulence model. Details of the numerical methods employed as well as the turbulence modelling adopted are given. Comparisons between experimental and numerical data are presented in terms of spanwise averaged trends of adiabatic effectiveness.

Nomenclature

A	Cross-section $[m^2]$	Re	Reynolds number $[-]$
BR	Blowing ratio $[-]$	Re_y	Near wall Reynolds number $[-]$
C	Oxygen concentration $[-]$	s_x	Streamwise pitch $[mm]$
d, D	Cooling hole diameter $[mm]$	s_z	Spanwise pitch $[mm]$
DR	Density ratio $[-]$	T	Temperature $[K]$
$EffCool$	Effusion Coolant Concentration $[-]$	U_i, U_j, U_k	Velocity components $[m\ s^{-1}]$
k	Turbulence kinetic energy $[m^2\ s^{-2}]$	$u_i^{'}, u_j^{'}, u_k^{'}$	Vel. comp. fluctuating parts $[m\ s^{-1}]$
L	Perforation length $[m]$	VR	Velocity ratio $[-]$
Le	Lewis number $[-]$	x, X	Streamwise direction $[m]$
$\dot{m}$	Mass flow rate $[kg\ s^{-1}]$	y, Y	Normal to the wall direction $[m]$
M	Molecular weight $[kg]$	y^+	Dimensionless wall distance $[-]$
Ma	Mach number $[-]$	z, Z	Spanwise direction $[m]$
P	Pressure $[Pa]$		

Greeks

γ	Anisotropic factor $[-]$	μ_t	Eddy viscosity $[kg\ m^{-1}\ s^{-1}]$
δ	Kronecker delta	ρ	Density $[kg\ m^{-3}]$
ε	Turbulence dissipation $[m^2\ s^{-3}]$	ω	Turbulence frequency $[s^{-1}]$
η_{ad}	Adiabatic effectiveness $[-]$		

Subscript

ad	Adiabatic	$main$	Mainstream
$cool$	Coolant	ref	Reference
eff	Effusion	w	Wall
fg	Foreign gas, N_2 or CO_2		

2. Experimental activity

2.1. Test case

The test rig, depicted in Fig. 1, is an open loop wind tunnel with a constant cross section area ($100 \times 100\ mm^2$; $1000\ mm$ long) which allows the complete control of two separate flows: the mainstream and the effusion cooling

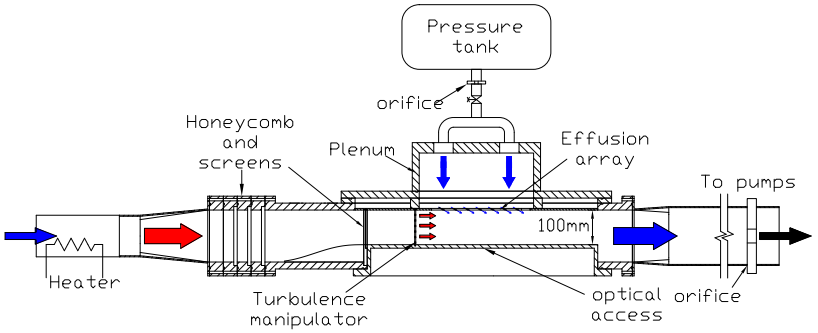

Fig. 1: Test rig scheme

flows. The mainstream is drawn by means of two vacuum pumps from the ambient with a maximum flow rate capability of about 900 m^3/h. In the first part of the channel the mainstream flow crosses honeycombs and several screens which allow to set an uniform velocity profile. An interchangeable passive turbulence generator (square grid mesh; 4 *mm* bar thickness; 16 *mm* grid pitch), located 64 *mm* upstream the effusion plate, is used to achieve a turbulence level of 17% at the first row of holes and a streamwise integral length scale of 7.5 *mm* (measured using a DANTEC® CTA system with a single sensor probe DANTEC® 55p04). The mean velocity measured upstream the first cooling row was uniform to within roughly 8% of the mean velocity, while turbulence intensity and integral length scale were uniform to within 15%. The test article is completely made of transparent PMMA (Poly-Methyl Methacrylate), thus allowing the required optical access for PSP (Pressure Sensitive Paint) measurements without influencing the UV excitation and the emission of the paint.

The effusion array is fed by a plenum chamber connected directly upstream the test plate with air, pure nitrogen or carbon dioxide stored in a pressure tank ($\approx 290\ K$); flow rate is set up by throttling the valves located on the cooling line. Two UV High Power Led 1 Watt filtered with a blue band bass filter provide the correct light source for PSP painted surface excitation, while a 1600×1200 resolution 14-bit CCD camera (PCO.1600) with a 610 *nm* red filter records the intensity emitted by PSP. Additional information on the test rig setup are reported in the work of Andreini et al.[21].

Pressure sensitive paint is an organic substance, composed by oxygen sensitive molecules embedded in the paint solution using a polymer binder permeable to oxygen. Based on luminescence behaviour of these molecules, PSP can be used to measure the oxygen concentration of the atmosphere surrounding the paints; in the recent years the pressure sensitive paint has been employed for highly detailed adiabatic effectiveness measurements exploiting the heat and mass transfer analogy [22]. PSP, made of a blend of Fluoro Isopropyl Butyl polymer (FIB) and Platinum tetra porphine (PtTFPP), are sprayed directly on the test surface (gas side of each effusion plates) with $6-8$ very light cross coats.

In the present work, one effusion geometry was considered: it represents a typical slanted effusion cooling scheme scaled up with respect to actual engine configurations. The hole spacing of the effusion plate is $s_x/d = 9.15$ and $s_z/d = 7.37$, where x is the streamwise direction and z is the spanwise direction. The hole diameter is 1.5 *mm*, the hole angle 30 deg and the length-to-diameter ratio of the film holes is 6.25. Perforations were manufactured by mechanical drilling on planar plates, resulting in cylindrical holes, and arranged in a staggered configuration with 18 rows of holes and 153 total number of holes.

The geometry has been tested imposing three different values of effusion Blowing Ratio and two values of Density Ratio, chosen within a typical range of aeroengine combustors; these parameters are defined as (along with the Velocity Ratio *VR*):

$$BR = \frac{\dot{m}_{eff}/\left(\pi \cdot n_{holes} \cdot d^2/4\right)}{\dot{m}_{main}/A_{main}}, \quad DR = \frac{\rho_{eff}}{\rho_{main}}, \quad VR = BR \cdot \frac{\rho_{main}}{\rho_{eff}} = \frac{BR}{DR} \tag{1}$$

where $\dot{m}_{eff}$ is the mass flow rate through the effusion plate; A_{main} is the mainstream channel cross-section ($100 \times 100\ mm^2$).

The cooling system was fed with carbon dioxide or pure nitrogen for adiabatic effectiveness measurements to reproduce respectively a $DR \approx 1.5$ and $DR \approx 1$, while air was used for the mainstream flow. The uncertainties of *BR* measurements are estimated to be ±5% with a confidence level of 95%. Mainstream absolute pressure was kept constant ($Re_{main} \approx 160000$ evaluated using the hydraulic diameter of the mainstream channel as reference length, $Ma_{main} \approx 0.07$), while coolant pressure was varied in order to ensure the desired values of coolant velocity inside the holes.

2.2. Experimental technique

Based on luminescence behaviour of Pressure Sensitive Paint molecules, PSP can be used to measure the oxygen concentration of the atmosphere surrounding the paints which in turn can be linked to the partial pressure of air: this property makes the paint suitable for gas concentration technique, based on the heat and mass transfer analogy [23], for adiabatic effectiveness measurements.

Despite the fact that the applicability of heat and mass transfer analogy has limitations, especially in case of

flowfields where viscous effects are dominating, it represents a good approximation for test cases as encountered in the present work [**?**]. Assuming valid the analogy, if a tracer gas without free oxygen is used as coolant in a film cooling system it is straightforward to replace the temperature definition of film cooling effectiveness by mass fractions of oxygen [23], and hence in terms of partial pressure of oxygen as measured with PSP [24]:

$$\eta_{ad} = \frac{T_{main} - T_{ad}}{T_{main} - T_{cool}} \equiv \frac{C_{main} - C_w}{C_{main}} = 1 - \frac{1}{\left(1 + \left(\frac{P_{O_2;air}/P_{O_2;ref}}{P_{O_2;fg}/P_{O_2;ref}} - 1\right)\frac{M_{fg}}{M_{air}}\right)} \tag{2}$$

where C_{main} and C_w are oxygen concentration respectively of main free stream and in proximity of the wall.

In order to evaluate the adiabatic effectiveness distribution using PSP technique, four types of images are needed for each tested flow condition:

1. the first image (*Dark Image*) is acquired with the UV illumination system switched off and it is necessary to correct the background noise of the camera;
2. using a tracer gas (N_2 or CO_2) for the cooling line and air for the mainstream, a second image is taken setting the desired flow conditions;
3. the third image is acquired imposing the same conditions of the previous one, but using air as coolant instead of nitrogen;
4. the last type of image is captured with no flow condition and it represents the reference intensity field of the measurements.

The four images can be used to estimate pixel by pixel the normalized partial pressure of oxygen in case of air or tracer gas injection (i.e. N_2 or CO_2) through holes array and hence to exploit the Eq. 2 to evaluate the effectiveness distribution. More information related to the experimental technique are extensively reported in the work of Caciolli et al.[22].

The estimate of the uncertainty of adiabatic effectiveness measurements was based on the method proposed by Kline and McClintock[25] and on a confidence level of 95%. It was estimated to be 10% for $\eta_{ad} = 0.2$ and 2% for $\eta_{ad} > 0.8$, taking into account the uncertainties in calibration and image capture. The adiabatic effectiveness tests were repeated several times in order to confirm the repeatability of the results.

3. Numerical setup

3D CFD RANS calculations have been considered in this study, referring to the Navier-Stokes solver ANSYS® CFX v14. The geometry of the test rig was replicated, including all the cooling rows. The mainstream boundary conditions have been assigned in terms of total pressure, total temperature and turbulence quantities at the main inlet, mass flow rate and total temperature are specified at the coolant inlet and mass flow rate was fixed at the outlet (Figure 2).

Compressibility effects was taken into account and a High Resolution advection scheme was used. Energy equation was solved in terms of total energy and viscous heating effects have been accounted for. Turbulence was modelled by

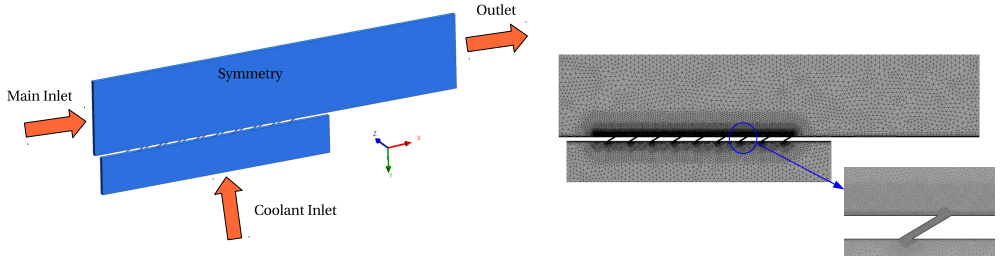

Fig. 2: Numerical domain (left) and grid (right).

means of the $k-\omega$ SST turbulence model, with an algebraic anisotropic correction suited to overcome typical RANS modelling failures for film cooling flows.

The selected near wall treatment uses an automatic blending between Wall Function and Wall Integration approach on the basis of y^+ value. For the cases presented in this work where $max(y^+) < 1$, the Low Reynolds formulation is always recovered.

Injections of both air and nitrogen were modelled with identical gas properties assuming ideal gas behaviour. From a dimensional analysis, the thermal field is totally driven by convection, so the effect of buoyancy was neglected both for $DR = 1$ and $DR = 1.5$. In order to track the coolant distribution, a transport equation for an additional passive scalar *EffCool* representing coolant concentration was solved: *EffCool* assumes the value 1 at the plenum inlet and 0 at the mainstream inlet. The value of its kinematic diffusivity was specified to guarantee a $Le = 1$ with the aim of fully respecting the mass-energy transfer analogy.

ANSYS ® ICEM-CFD has been used to generate hybrid computational grids (tetrahedral with 15 layers of prisms close to the wall). In order to reduce the computational cost, it has been decided to take advantage of the symmetry condition offered by the geometry (see Figure 2). In this way, only half hole has been modeled for each row. It is well known that mesh refinement plays a central role in film cooling simulations. A comprehensive mesh sensitivity analysis, described in details in [26], identified in a grid characterized by 7.4 million of elements the best compromise to correctly catch the local concentration gradients at an affordable computational cost.

The solution convergence has been assessed by monitoring that rms residuals fell below a prescribed value of $1E-6$ and verifying that the averaged value of η_{ad} on the plate reached a steady-state.

3.1. Anisotropic correction

It is known [27] that standard RANS numerical computations exploiting eddy viscosity assumption fails to correctly predict the jet in crossflow mixing and development. This is due to the assumption of turbulence isotropy that fails in the near-wall region because of the damping of normal to wall fluctuations and the neglecting of all unsteady interactions between the two streams.

Andrei et al.[28] reviewed a set of turbulence models specifically developed for film and effusion cooling applications, showing how, at low and moderate blowing ratios, an improvement of predictive capabilities can be obtained considering a tensorial definition of the eddy viscosity and doping the stream-spanwise components to augment lateral jet diffusion as suggested in [16].

In a recent work [26], the algebraic anisotropic correction tested in [28] was implemented in the commercial ANSYS® CFX solver by means of source terms in the conservation equations and tested against standard isotropic $k-\omega$ SST turbulence model, showing a very good capability to represent experimental data provided by Andreini et al.[21], especially in case of slanted perforation.

A brief description of the implemented corrections are reported in this section. For further details, refer to [28] and [26].

The basic idea is to calculate the Reynolds Stress tensor:

$$-\rho\overline{u_i' u_j'} = \mu_{t,ij}\left(\frac{\partial U_i}{\partial x_j}+\frac{\partial U_j}{\partial x_i}-\frac{2}{3}\delta_{ij}\frac{\partial U_k}{\partial x_k}\right), \tag{3}$$

where turbulent viscosity is augmented for the stream-span directions by an amplification factor γ:

$$\mu_{t,ij} = \begin{pmatrix} \mu_t & \mu_t & \gamma\mu_t \\ \mu_t & \mu_t & \mu_t \\ \gamma\mu_t & \mu_t & \mu_t \end{pmatrix} \tag{4}$$

The value for the anisotropic correction γ follows the correlation in Eq. 5 bounded to the upper and lower limits of 60 and 4.5, for $y^\star < 1.5$ and outside the buffer layer respectively [29]. The lower bound corresponds to the asymptotic value at the edge of the boundary layer as measured by Kaszeta and Simon [30], while the upper bound inside the viscous sub-layer is suggested by Azzi and Lakehal [29] to prevent numerical instabilities arising in case of small $y^\star$ due to negative values of γ:

$$\gamma = \frac{1000 y^{\star 0.42}}{2.682 y^{\star 2} - 5.463}, \text{ where } y^\star = 0.00442 Re_y^2 + 0.294 Re_y + 0.545 \tag{5}$$

This function was proposed by Lakehal[31] to match DNS simulations of turbulent flat plate by Kim et al.[32].

The proposed correction is applied to the domain of the evolving jet only, thus isotropic formulation is recovered inside the coolant plenum, within the perforations and outside the boundary layer in the main duct.

The above described anisotropic modification was firstly inserted in the framework of $k-\omega$ SST model Cottin et al.[17] and subsequently tested by the authors in [28]. The anisotropic correction is introduced by means of additional source terms (conventionally taken on the right hand side of the conservation equations) modelling turbulent flux modification in the momentum, energy, turbulence and passive scalar transport equations.

4. Experimental and numerical results

In Fig. 3 the bidimensional adiabatic effectiveness distributions are shown for all the tested blowing ratios; analysis of the film cooling performance can be conducted using lateral averaged adiabatic effectiveness distributions against BR. Considering the $DR = 1$ case, as shown in Figure 4, the highest film wall protection is achieved at low blowing ratio for $x/S_x < 6$, whereas opposite behaviour is reported for the remaining part of the plate. This behaviour can be attributed to the lift-off of the coolant jets, which does not guarantee a correct wall protection at the first rows of holes, while after the sixth row and for higher blowing ratio values, the large amount of coolant mass flow injected and the superposition effect lead to an higher adiabatic effectiveness. In addition, an asymptotic condition seems to be reached at $BR = 1$ and as shown by the 2D distributions the coolant jets work in penetration regime at all the imposed values of blowing rate. The poor film protection in the first rows of holes emphasizes the necessity of a starter film, especially in presence of a radiative load.

On the other hand, the $DR = 1.5$ case, more representative to the actual engine condition, is subject to a lower effective velocity ratio: in fact at $BR = 1$ the regime switches from penetration to mixing respect to the $DR = 1$ case described above. This phenomena, clearly evident from the shape of coolant traces, guarantees for $BR = 1$ the higher film protection up to $x/S_x = 14$.

Concerning the influence of the density ratio (Figure 5), experiments show that for $BR > 1$, η_{ad} generated by the effusion jets is weakly affected by DR. This suggests that, within the penetration regime, the effects of density ratio can be practically neglected and the film performances are well described by the blowing rate. However, as stated above, at $BR = 1$ changing the DR the jets work in different regime and as a consequence the effectiveness results deeply influenced by the DR, especially for the first rows of holes where the difference in the effective density ratio is more pronounced. It is worth noticing that, according to the classification introduced by L'Ecuyer and Soechting[20], the present test matrix does not allow to point out the effect of DR in the mixing and mass addiction regime.

Figure 6 reports the comparisons between experimental and numerical data for the three different BR values. Concerning $DR = 1$ cases, numerical model well predicts spanwise averaged adiabatic effectiveness in terms of both trend and values, especially at higher BR, where a relative error below 10% is achieved. The agreement slightly worsens at $BR = 1$, leading to a general overestimation of η_{ad}, especially moving toward the end of the plate. As reported in [26], the anisotropic model predictions result in a lower jet penetration and in a less pronounced kidney-

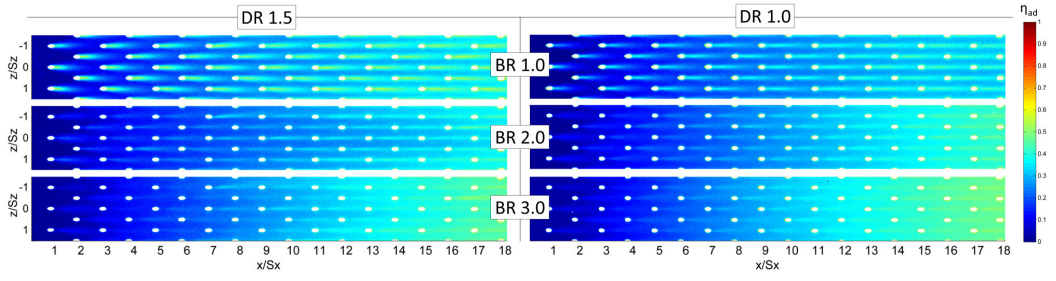

Fig. 3: Experimental adiabatic effectiveness distributions on the effusion plate.

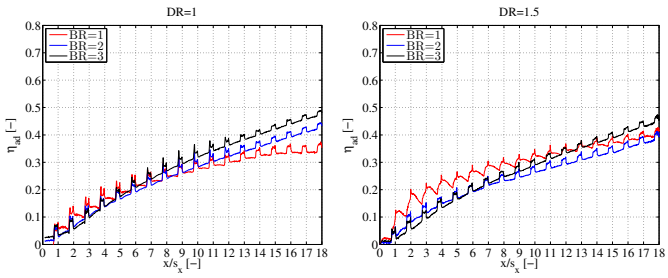

Fig. 4: Experimental results: *BR* effects on adiabatic effectiveness.

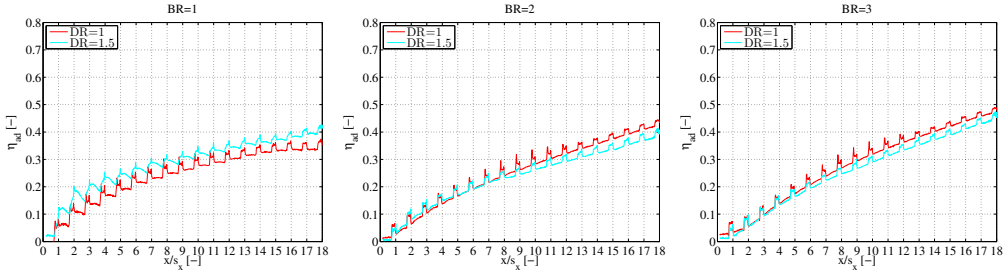

Fig. 5: Experimental results: *DR* effects on adiabatic effectiveness.

vortex which is responsible for the ingestion of hot gas below the jet itself. In such a way the entire region within the two symmetry planes shows a higher film protection due to a more complete merging of consecutive jets.

For the $DR = 1.5$ cases (representing conditions that are more representative than the previous ones), looking at higher *BR* condition, a slight worsening of the agreement can be noticed, with a gap that remains nearly constant up to the end of the plate. The same trend was not obtained for $BR = 1$, in which case the overestimation becomes relevant already from the first rows. This result can be ascribed to the misprediction of the regime, as can be noticed comparing the slope of η_{ad} curves on the first rows, which is completely different between numerical and experimental data. CFD simulation returns an increasing trend, typical of the penetration regime, whereas experiments highlight higher peak values, balanced by a sudden decay typical of mixing regime.

In order to better understand the flow characteristics in the investigated conditions, concentration contour plot on the symmetry plane are presented in Figure 7, focusing on the 1^{st} and 13^{th} rows of holes. Flow conditions are largely sensitive to *BR*, whereas the *DR* has a significant effect only at low *BR* values. As already hinted, penetration regime is reported also for $BR = 1$, where, even though the jets are actually confined in a thin layer along the wall, no reattachment to wall is visible, as highlighted in Figure 6 by the increasing slope of the first rows.

5. Conclusions

A comprehensive analysis has been carried out in order to investigate the adiabatic effectiveness performance of a multi-perforated planar plate representative of effusion cooled combustor liners, both from an experimental and a numerical point of view. The selected test case represents a severe benchmark for the numerical models that have to cope with complex turbulent flow field and mixing phenomena due to the multiple coolant injections. Adiabatic effectiveness tests were carried out using Pressure Sensitive Paint Technique, at high turbulence conditions, blowing ratio values ranging from 1 to 3 and density ratio values from 1 to 1.5. Numerical simulations have been conducted exploiting an algebraic anisotropic correction to $k - \omega$ SST turbulence model in order to overcome the well known jet penetration overprediction and lateral spreading underestimation of classical RANS turbulence modelling.

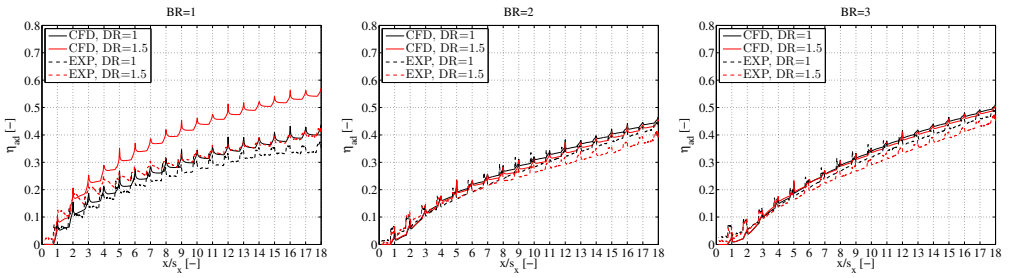

Fig. 6: Comparisons between numerical and experimental data.

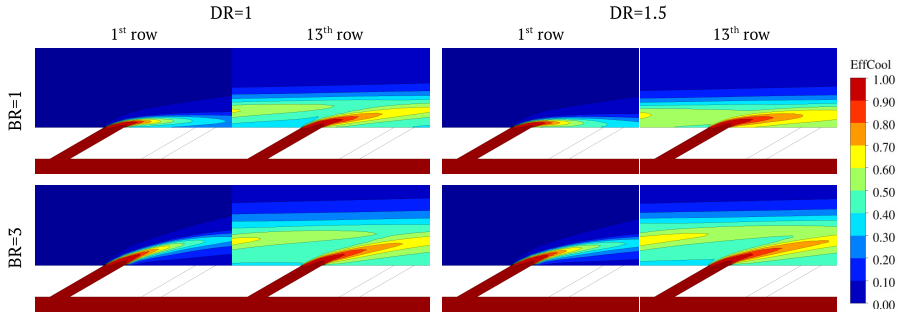

Fig. 7: *Effcool* contour plot on symmetry plane.

Detailed measurements of film effectiveness pointed out the effect of the different flow conditions. The higher film wall protection is achieved at low blowing ratio in the first part of the plate (up to $x/S_x < 6$) due to jets lift-off, whereas opposite behaviour is reported for the final part where the superposition effect prevails. Regarding the role of density ratio, this parameter influences the film covering only in the mixing regime, while its effect in the penetration regime can be neglected. Numerical predictions showed to be able to correctly predict the experimental trends connected with increasing *BR* and *DR* values. In particular, the effects of Density Ratio variations are captured, returning the opposing effects varying the Blowing Ratio showed by experiments. An underestimation of jets penetration due to RANS modelling has been noticed at every condition, whose effect is however very dependent: a good agreement has been achieved in the full penetration regime, whereas at low *BR* a slight misprediction of the film cooling regime leads to a huge overprediction in terms of adiabatic effectiveness.

Acknowledgements

The authors wish to gratefully acknowledge KIAI (Knowledge for Ignition, Acoustics and Instabilities) Consortium for the kind permission of publishing the results herein. KIAI is an EU funded Research Project within the 7th Framework Programme.

References

[1] Andrews, G.E., Bazdidi-Tehrani, F., Hussain, C.I., Pearson, J.P.. Small diameter film cooling hole heat transfer: The influence of hole length. ASME Paper 1991;91-GT-344.

[2] Andrews, G.E., Khalifa, I.M., Asere, A.A., Bazdidi-Tehrani, F.. Full coverage effusion film cooling with inclined holes. ASME Paper 1995;95-GT-274.

[3] Scrittore, J.J., Thole, K.A., Burd, S.. Experimental characterization of film-cooling effectiveness near combustor dilution holes. ASME Turbo Expo 2005;GT2005-68704.
[4] Facchini, B., Maiuolo, F., Tarchi, L., Coutandin, D.. Experimental investigation on the effects of a large recirculating area on the performance of an effusion cooled combustor liner. J Eng Gas Turbines and Power 2012;134(4):041505 (pages 9). doi:10.1115/1.4004729.
[5] Ligrani, P., Goodro, M., Fox, M., Moon, H.K.. Full-coverage film cooling: Film effectiveness and heat transfer coefficients for dense and sparse hole arrays at different blowing ratios. J TURBOMACH 2012;134(6):061039 (pages 13). doi:10.1115/1.4006304.
[6] Martin, A., Thorpe, S.J.. Experiments on combustor effusion cooling under conditions of very high free-stream turbulence. ASME Conference Proceedings 2012;(GT2012-68863).
[7] Lin, Y., Song, B., Li, B., Liu, G.. Investigation of film cooling effectiveness of full-coverage inclined multihole walls with different hole arrangements. ASME Journal of Heat Transfer 2006;128(GT2012-68863):580–585.
[8] Andreini, A., Caciolli, G., Facchini, B., Tarchi, L.. Experimental evaluation of the density ratio effects on the cooling performance of a combined slot/effusion combustor cooling system. ISRN Aerospace Engineering 2013;2013(423190). doi:10.1155/2013/423190.
[9] Crabb, D., Durao, D.F.G., Whitelaw, J.H.. A round jet normal to a crossflow. Trans ASME: J Fluids Eng 1981;(103).
[10] Galeazzo, F.C.C., Donnert, G., Habisreuther, P., Zarzalis, N., Valdes, R.J., Krebs, W.. Measurement and simulation of turbulent mixing in a jet in crossflow. Proceedings of ASME Turbo Expo 2010;(GT2010-22709).
[11] Mendez, S., Nicoud, F.. An adiabatic homogeneous model for the flow around a multi-perforated plate. AIAA Journal 2008;10(46):2623–2633.
[12] Hoda, A., Acharya, S.. Predictions of a film coolant jet in crossflow with different turbulence models. ASME J Turbomach 2000;122:558–569.
[13] Harrison, K.L., Bogard, D.G.. Comparison of RANS turbulence models for prediction of film cooling performance. Proceedings of ASME Turbo Expo 2008;(GT2008-51423).
[14] Bacci, A., Facchini, B.. Turbulence modeling for the numerical simulation of film and effusion cooling flows. Proceedings of ASME Turbo Expo 2007;(GT2007-27182).
[15] Holloway, D.S., Walters, D.K., Leylek, J.H.. Computational study of jet-in-crossflow and film cooling using a new unsteady-based turbulence model. Proceedings of ASME Turbo Expo 2005;(GT2005-68155).
[16] Bergeles, , Gosman, G., Launder, A.D.. The turbulent jet in a cross stream at low injection rates: a three-dimensional numerical treatment. Numerical Heat Transfer 1978;1:217–242.
[17] Cottin, G., Laroche, E., Savary, N., Millan, P.. Modeling of the heat flux for multi-hole cooling applications. Proceedings of ASME Turbo Expo 2011;(GT2011-46330).
[18] Li, X., Ren, J., Jiang, H.. Algebraic anisotropic eddy-viscosity modeling application to the turbulent film cooling flows. Proceedings of ASME Turbo Expo 2011;(GT2011-45791).
[19] Walters, D.K.. Development of novel turbulence modeling techniques for turbomachinery applications. Clemson University, PhD thesis 2000;.
[20] L'Ecuyer, M.R., Soechting, F.O.. A model for correlating flat plate film-cooling effectiveness for rows of round holes. AGARD-CP-390 1985;.
[21] Andreini, A., Facchini, B., Picchi, A., Tarchi, L., Turrini, F.. Experimental and theoretical investigation of thermal effectiveness in multi-perforated plates for combustor liner effusion cooling. Proceedings of ASME Turbo Expo 2013;(GT2013-94667).
[22] Caciolli, G., Facchini, B., Picchi, A., Tarchi, L.. Comparison between {PSP} and {TLC} steady state techniques for adiabatic effectiveness measurement on a multiperforated plate. Experimental Thermal and Fluid Science 2013;48(0):122 – 133. doi:http://dx.doi.org/10.1016/j.expthermflusci.2013.02.015.
[23] Jones, T.V.. Theory for the use of foreign gas in simulating film cooling. International Journal of Heat and Fluid Flow 1999;20:349–354.
[24] Charbonnier, D., Ott, P., Jonsson, M., Cottier, F., Köbke, T.. Experimental and numerical study of the thermal performance of a film cooled turbine platform. ASME Conference Proceedings 2009;GT2009-60306(48845):1027–1038. doi:10.1115/GT2009-60306.
[25] Kline, S.J., McClintock, F.A.. Describing uncertainties in single sample experiments. Mechanical Engineering 1953;75:3–8.
[26] Andrei, L., Andreini, A., Bianchini, C., Facchini, B., Mazzei, L.. Numerical analysis of effusion plates for combustor liners cooling with varying density ratio. Proceedings of ASME Turbo Expo 2013;(GT2013-95039).
[27] Azzi, A., Jubran, B.A.. Numerical modeling of film cooling from short length stream-wise injection holes. Heat and Mass Transfer 2003;39:345–353.
[28] Andrei, L., Andreini, A., Bianchini, C., Facchini, B.. Numerical benchmark of non-conventional rans turbulence models for film and effusion cooling. ASME J Turbomach 2013;.
[29] Azzi, A., Lakehal, D.. Perspectives in modeling film cooling of turbine blades by transcending conventional two-equation turbulence models. ASME J Turbomach 2002;124:472–484.
[30] Kaszeta, R.W., Simon, T.W.. Measurement of eddy diffusivity of momentum in film cooling flows with streamwise injection. ASME J Turbomach 2000;122:178–183.
[31] Lakehal, D.. Near-wall modeling of turbulent convective heat transport in film cooling of turbine blades with the aid of direct numerical simulation data. ASME J Turbomach 2002;124:485–498.
[32] Kim, J., Moin, P., Moser, R.. Turbulence statistics in fully developed channel flow at low reynolds number. J Fluid Mech 1987;177:133–166.